Mechanisms of Bonding Effected by Nanoparticles in Zirconia Coatings Applied by Spraying of Suspensions

J. Adam, M. Aslan, R. Drumm, M. Veith

[20] T. Sugimoto, in Monodisperse Particles, Elsevier, Amsterdam, Netherlands 2001.

[21] N. Nitin, L. E. W. LaConte, O. Zurkiya, X. Hu, G. Bao, J. Biol. Inorg. Chem. 2004, 9, 706.

[22] Z. Liu, D. Zhang, S. Han, C. Li, B. Lei, W. Lu, J. Fang, C. Zhou, J. Am. Chem. Soc, 2005, 127, 6.

[23] J. Wang, Q. Chen, C. Zeng, B. Hou, Adv. Mater. 2004, 16, 137.

[24] J. R. Morber, Y. Ding, M. S. Haluska, Y. Li, J. P. Liu, Z. L. Wang, R. L. Snyder, Phys. Rev. B 2006, 110, 21672.

[25] J. Bachmann, J. Jing, M. Knez, S. Barth, H. Shen, S. Mathur, U. Goesele, K. Nielsch, J. Am. Chem. Soc. 2007, 129, 9554.

[26] (a) S. Mathur, M. Veith, V. Sivakov, H. Shen, V. Huch, U. Hartmann, H. B. Gao, Chem. Vap. Depos. 2002, 8, 277; (b) S. Mathur, V. Sivakov, H. Shen, S. Barth, C. Cavelius, A. Nilsson, P. Kuhn, Thin Solid Films 2006, 502, 88; (c) S. Mathur, H. Shen, V. Sivakov, U. Werner, Chem. Mater. 2004, 16, 2449.

[27] D. M. Lind, S. D. Berry, G. Chern, H. Mathias, L. R. Testardi, Phys. Rev. B 1992, 45, 1838.

[28] (a) S. Mathur, S. Barth, U. Werner, F. Hernandez-Ramirez, A. Romano-Rodriguez, Adv. Mater. 2008, in print; (b) S. Mathur, S. Barth, Z. Phys. Chem. 2008, 222, 307.

[29] M. Bohra, N. Venkataramani, S. Prasad, N. Kumar, D. S. Misra, S. C. Sahoo, R. Krishnan, J. Magn. Magn. Mater. 2007, 310, 2242.

[30] (a) A. Vorniero, M. Ferroni, E. Comini, G. Fagkia, G. Sberveglieri, Nano Lett. 2007, 7, 3553; (b) L. Xu, Y. Su, S. Li, Y. Q. Chen, Q. T. Zhou, S. Yin, Y. Feng, Phys. Chem. B 2007, 111, 760.

[31] J. E. Evans, K. W. Springer, J. Z. Zhang, J. Chem. Phys. 1994, 101, 6222.

Mechanisms of Bonding Effected by Nanoparticles in Zirconia Coatings Applied by Spraying of Suspensions

Abstract

Zirconia coatings consisting of a mixture of coarse and fine grained zirconia powders prepared by spraying of suspensions and subsequent thermal treatment at limited temperatures (up to 500°C) are poor in adherence and in intrinsic mechanical strength. We have shown elsewhere that mechanical properties of these coatings can be improved clearly by adding a small amount of nanoscaled zirconia.

Here, the structural and the chemical development of this coating material and of the nanoparticles is examined to gain information about the underlying bonding mechanisms. The applied temperature is relatively low in comparison to the usual onset temperature of accelerated sintering. Nevertheless, the results show that diffusion controlled material transport mechanisms play their role in bonding. The condensation of surface OH groups may participate in bonding, too.

These first results confirm the potential of nanoparticles to act as inorganic binder. Additional research effort to clarify the underlying mechanisms in detail is of interest. For the practical side, it can be concluded that the resulting effect of mechanical consolidation of ceramic structures at relatively low temperatures enables new ceramic applications, for example a new type of ceramic coatings on metallic substrates.

Keywords: ZrO_2, ceramic coatings, nanoparticles, bonding, colloidal processing.

Introduction

Different surface functionalities can be realised on metals by thick ceramic coatings. PVD/CVD and sol-gel routes lead to a limited coating thickness. Usually coatings with a thickness in the order of 100 µm are applied by using high temperature processes. Corresponding main routes are enamelling and various thermal spraying processes [1]. These coatings are also suitable for long term operation at high temperatures. When coating methods on the basis of particle suspensions with subsequent heat treatment are used, drying and sintering shrinkage are detrimental effects on formation of dense and well adhering coatings on rigid substrates.

One approach to reduce shrinkage is to include fractions of larger particles. Lan and Xiao [2] minimized drying stress and cracking of ZrO_2 coatings during drying by adding sub-µm or µm particles to a suspension of nanoparticles. Their colleagues, Wang et al. [3] avoided overall shrinkage with the so-called ‘bricks and mortar’ concept using 10-60 µm ZrO_2 particles as structural backbone. The coatings with a thickness of 200-600 µm were fired at 1200°C with the ‘mortar’ consisting of 14 nm ZrO_2 particles to obtain mechanical strength.

However, many substrates do not allow such high heat treatment temperatures. Applications that require neither sophisticated coating strengths nor dense coatings would be simply and economically accessible by colloidal coating methods (dipping, spin coating, spraying) if bonding could be realised at low application temperatures. At 500°C we achieved ZrO_2 coatings with a remarkable strength if ~ 8 wt.-% of the ceramic fraction consisted of nanoparticles [4]. This interesting result directly leads to the question about the underlying bonding mechanisms.

Surface diffusion is the first expected sintering mechanism in the low temperature sintering stage. A rough estimation of the onset temperature of surface diffusion is given by the “Hüttig temperature” $T_H = 0.3 \cdot T_{melt}$ (T in K) which is 620°C in the case of ZrO_2. Akash [5] determined the temperature dependence of the surface diffusion coefficient in the temperature range of 900-1050°C for yttria stabilized zirconia particles with a mean particle size of 15 nm, determined by XRD/Scherrer equation. Extrapolating the surface diffusion coefficient given by Akash down to a temperature of 500°C results in a massively smaller surface diffusion coefficient (13 orders of magnitude lower). At first sight, it can be concluded from this extrapolation and from the Hüttig temperature, that surface diffusion should not be relevant at 500°C. But, the results of Skandan [6] show that the impact of particle size on sintering in the lower nm-range has to be considered. Compacts made of 6 nm zirconia particles exhibit a linear dilatometric shrinkage of ~ 2 % [6] with increasing temperatures up to 500°C due to coarsening and particle rearrangement. Particle coarsening and shrinkage give the hint that diffusion is relevant at 500°C for particles < 10 nm. Next to surface diffusion even volume and grain boundary diffusion would take place because these two mechanisms are connected with shrinkage. Other work [7] confirms by specific surface area measurements, XRD and TEM that ZrO_2 particles in the same size range are coarsening with increasing calcination temperatures from 400 to 450 and 600°C. For example from XRD data crystallite sizes of 6, 8, 11 nm for the respective temperatures were calculated.

Coalescence has to be mentioned as a further particle coarsening mechanism. In-situ TEM observations at 890°C revealed this mechanism for 20-200 nm zirconia particles next to formation of sintering necks [8].

Physisorbed and chemisorbed surface water becomes quantitatively relevant for nanoparticulate powders because of their high specific surface area. For their study the authors of [9] annealed ZrO_2 powder with a specific surface area of 80 m^2/g at 600°C to remove organics. Then, they found a reversible water uptake of 2.5 wt.-% from air as determined by weight loss up to 400°C by TG analysis. In agreement with this result and on the basis of quasielastic neutron scattering experiments, they conclude the existence of two hydration layers on top of the layer of surface OH groups. The number of layers results from the assumed areal density of about 4.6 molecules per nm^2 which was a cited literature value, given for silica surfaces. The question arises if a higher water amount could have been found if final TG analysis temperature had been higher. A report [10] leads to this conclusion because their FTIR spectral analysis shows that OH groups are still present on zirconia surfaces after heat treatment at 400°C under vacuum.

Anyway, several OH groups per nm^2 are present on zirconia surfaces representing an amount being worth to consider when nanoparticles are used generally. Dehydration alters chemical bonds and is also causing material transport. So, it may contribute to the formation of interparticle bonds, as will be discussed.

The present work investigates the chemical and microstructural development of coatings based on a nanoparticulate "mortar" in a temperature range up to 500°C in order to identify possible bonding mechanisms in our coatings [4].

Experimental

In our work we compare the behaviour of a) the pure ZrO_2 nanoparticle fraction ("n-ZrO$_2$") and b) the coating material (termed as the "mix") that did not undergo thermal consolidation at 500°C prior to the examinations.

The n-ZrO$_2$ (doped with 4 mole-% Y_2O_3) was produced by a precipitation and hydrothermal treatment. Afterwards, as continuation of the nanoparticle preparation process [11], the particles were chemo-mechanically surface modified to obtain stable colloids (d_{50}(vol) = 14 nm) in ethanol. XRD reveals tetragonal crystallites with an average size of 6.1 nm. A specific surface area of 164 m^2/g can be calculated ($Aspec = 6000 / [d_{XRD} \cdot \rho]$) from this value which is in good agreement with BET measurements: 166 m^2/g for the powder being free of organics.

The ethanolic suspension for the spray application of the coatings contained 80 wt.-% ZrO$_2$ and 1.3 wt-% 3,6,9-trioxadecanic acid as surface modifier / dispersing agent. The ceramic fraction consisted of 65.8 wt.-% calcined spray dried granules (Tosoh TZ-3Y, exhibiting 4.6 m^2/g after calcination at 1200°C), 26.3 wt.-% of de-agglomerated ZrO$_2$ (Tosoh TZ-3Y, 13.5 m^2/g) and 7.9 wt.-% of n-ZrO$_2$. This suspension was sprayed on steel substrates, dried, and the coating was removed to gain the "mix". For the results in [4] the coatings have been consolidated at 500°C and it is shown there that their abrasion resistance is clearly higher, in comparison to coatings without nanoparticles. Further details on suspension and coating preparation can be found in [4].

Here, the mix and n-ZrO$_2$ were examined by …

- Dilatometry - Linseis "Dilatometer L25". Samples have been compacted without binders or pressing additives by axial and isostatic pressing, 10 K/min heating rate in the dilatometer
- N2 ad-/ desorption - Quantachrome "Autosorb-AS6", for BET specific surface area determination and to receive the BJH pore size distribution
- TG/DSC - Netzsch "STA 449 C", 10 K/min heating rate, in air atmosphere
- C/H analyser (carrier hot gas extraction method) - Leco "RC-412", 50 K/min heating rate
- XRD - Philips "X'Pert MRI"

Results and Discussion

Sintering shrinkage measurements as well as measurements to determine the development of the specific surface area and of the pore structure have been executed to allow conclusions about sintering mechanisms. The accompanying characterization of mass loss, heat flow and C/H release completes the examinations on the side of chemical reactions taking place upon heating the material up to 500°C.

1 Dilatometry

Shrinkage curves of the mix and n-ZrO$_2$ are shown in figure1. Due to the use of a coarse ZrO_2 fraction (calcined granules in the size range 10-100 µm) the mix material does not undergo relevant shrinkage, even up to 1000°C, which is an important requirement to receive crack free and adhering coatings on a rigid substrate.

In contrast, the shrinkage of n-ZrO_2 starts above 200°C and passes to accelerated sintering at about 900°C. This broad temperature range of first linear shrinkage and the observed shrinkage of 3.2 % at 500°C leads to the conclusion that material transport mechanisms (particle rearrangement, diffusion) take place. Thus, neck growth and shrinkage are relevant for n-ZrO_2 at 500°C, although those mechanisms appear at much higher temperatures for sub-µm particles.

The coarsening of n-ZrO_2 particles is confirmed by XRD measurements (6.1 → 7.8 nm after heat treatment at 500°C). From dilatometry it can be concluded that nanoparticles themselves can undergo shrinkage at comparatively low temperatures. Therefore, nanoparticles in the coatings being in contact with larger particles can act as binding bridges by the formation of sintering necks without shrinkage. The binding effect of the nanoparticles can be explained on the basis of material transport mechanisms that have been proven indirectly by dilatometry, XRD and specific surface area measurements, as will be shown in the next section.

2 Specific surface area and pore size

The specific surface area of the n-ZrO_2 decreases from 166 m^2/g at room temperature to 115 m^2/g at 500 °C (table 1). The reduction of the specific surface area is in good agreement with the theoretical values calculated from XRD data due to particle coarsening and formation of particle contact areas that are not longer accessible for N_2 adsorption.

n-ZrO_2	calculated from XRD data	measured
RT	6.1 nm →164 m^2/g	166 m^2/g (a)
500°C	7.8 nm → 128 m^2/g	115 m^2/g

Table 1: Specific surface area of n-ZrO_2.(a): mean value of measurements on 2 samplesafter stripping off organics

Table 2 summarises specific surface areas for the mix. Values slightly above 21 m^2/g have been measured. The calculated value was obtained by adding the weighted

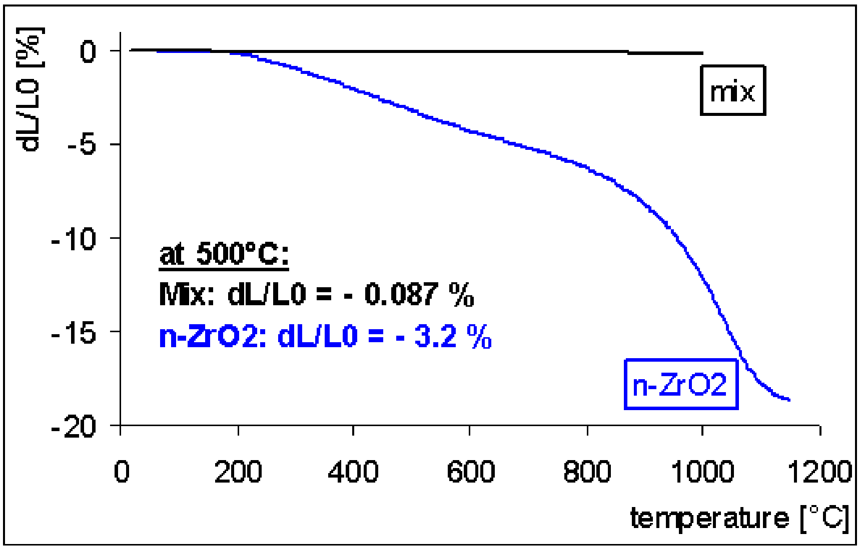

Fig. 1: Linear shrinkage of mix and n-ZrO_2, dilatometric measurement (see text for specification of mix).

areas of the ZrO_2 fractions. The fact that measured values are higher than the calculated values can be explained by a slight sedimentation of coarse zirconia granules in the suspension prior spray application and their resulting depletion in the coating. This effect probably causes variations of the fractional ZrO_2 coating composition which may also result in variations of surface areas. Another factor influencing surface area measurements can be given by the presence of organics (1.6 wt.-% = 6.2 vol.-% surface modifier). To check if the organic fraction masks a part of the surface area, the mix was cleaned/washed with Na(OH) to strip off the organics. The so treated mix exhibits a larger surface area of 23.8 m^2/g. Compared to the value after heat treatment at 500°C, it results in an apparent decrease of surface area. This is a hint to conclude that surface reducing sintering mechanisms can also be present in the mix. But, regarding the discussed possible compositional variations, this conclusion has to be made with care.

Mix	measured	calc. from comp.
RT	21.1(b) / 23.8(c) m^2/g	19.7 m^2/g
500°C	21.6 m^2/g	15.7(d) m^2/g

Table 2: Specific surface area of the mix. (b): with organics, (c): free of organics, (d) used value for n-ZrO_2: 115 m^2/g (see text for specification of mix).

Increase in pore volume and average pore size (11.3 → 13.7 nm) can be observed in figure 2, when the mix in room temperature state / after heating to 500°C is compared (figure 2). On the basis of present results, it cannot be concluded if this is due to organics burn out and/or due to sintering neck formation and "pore smoothing" [5].

A complete disappearance of the micropores (< 2 nm) being present in the room temperature state of the mix give a strong hint for sintering neck formation and/or coalescence of particles at 500°C.

3 DSC / TG measurements

Figure 3 shows the DSC and TG plots of the mix upon heating. There is one exothermic DSC peak at 333°C which can be ascribed to organics burn out and correlates to the mass loss in this temperature range. A further step of mass loss below 200°C can be explained with the loss of adsorbed water.

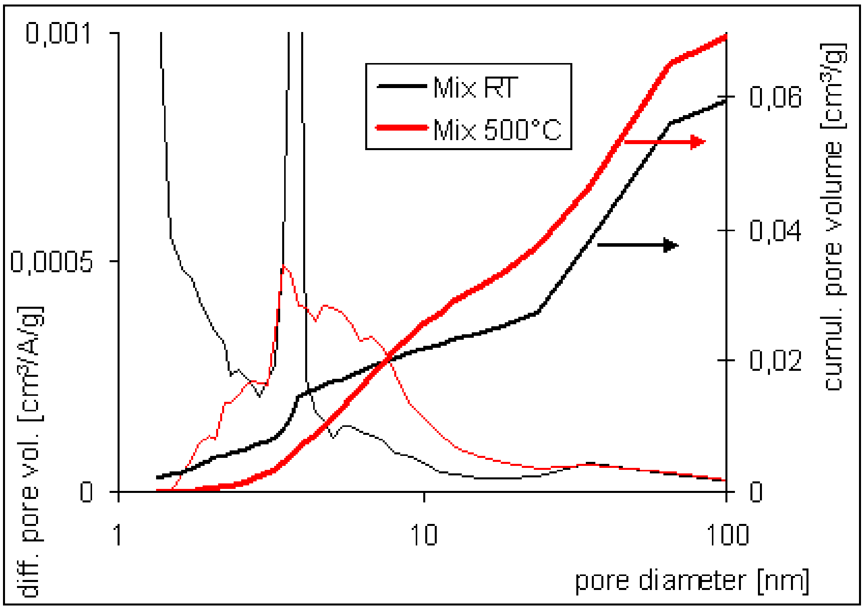

Fig.2: Differential and cumulative pore volume distributions in the mix (see text for specification of mix).

4 C/H analyser

The DSC and TG data can be underlined by measurements with the C/H analyser, as shown in figure 4. Here, the appearance of carbon coming from the sample shows a maximum at 287°C. This lower peak temperature can be explained by the use of pure oxygen as analysis gas in comparison to air in the DSC/TG.

Water originates from different sources like water adsorbed on the surface and in the pores (appears at lower temperatures than C), from oxidized H from organics (signal decreases parallel to that of C) and from surface OH groups (at higher temperatures). Considering a C content of 50 wt.-% and a H content of 10.5 wt.-% in the organics (this is close to the values of the surface modifier and of potential residual ethanol in the pores), it is possible to allocate 2.7 wt.-% of the measured water to the organics. From two Karl-Fischer titrations, a mean content of adsorbed water in the mix of 0.44 wt.-% was determined. Subtracting this physisorbed water and the amount of water due to organics from the total measured water amount (3.54 wt.-%) leads to the result that 0.4 wt.-% water may have surface hydroxyl groups as origin.

This equals to 11 OH groups per nm^2 of the ZrO_2 surface area, which is significantly higher than given in literature (4.6 OH groups / nm^2) [9]. These authors assumed the existence of three layers with this density and stated that the adsorbed H_2O layers being directly on the layer of OH groups are very immobile, too. So, these inner immobile adsorbed water layers may not be detected by the Karl Fischer method. This is a possible reason why we found a higher number of surface OH groups.

Anyway, from this calculation and the general state of knowledge the existence of several OH groups per nm^2 on surfaces of oxides can be taken as fact. As they become quantitatively relevant for nanoparticles with e.g. surface areas > 100 m^2/g, this publication suggests to consider their role in binding effects by nanoparticles. At low temperatures where diffusion mechanisms are not yet relevant, binding could take place as condensation of OH groups to form Me-O-Me bonds (Me = metal).

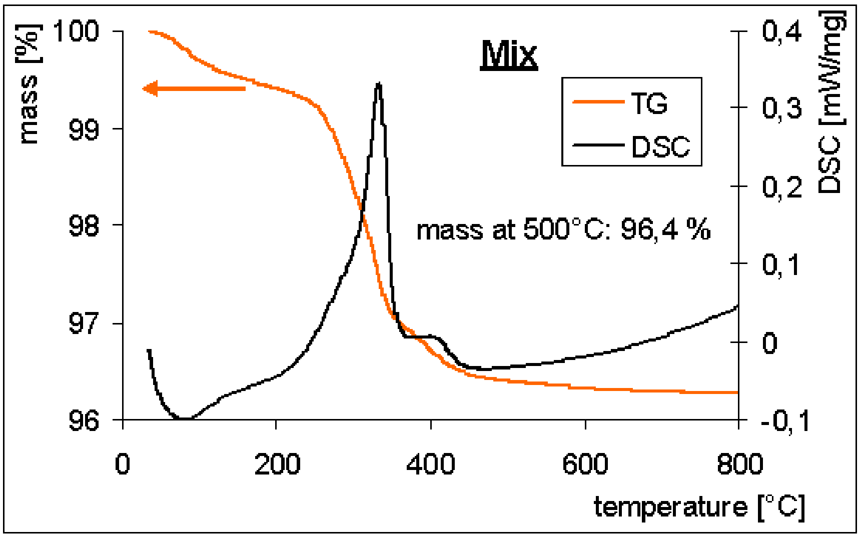

Fig. 3: Thermo-gravimetric and differential scanning calorimeter signal of the mix (see text for specification of mix).

Conclusions

The remarkable bonding effect [4] of ~ 8 wt.-% zirconia nanoparticles in ZrO_2 coatings that have been heat treated at 500°C is examined and discussed for the first time. For this temperature, in agreement with the literature it was concluded that sintering mechanisms are active for the nanoparticles used, even those mechanisms that cause grain coarsening and shrinkage locally. Further, the condensation of surface hydroxyl groups may contribute to inter particle bonding. This effect may be superimposed by sintering.

More research is needed to identify and quantify the relevant bonding mechanisms in detail. Further information would be gained if neck growth and/or coalescence of ~ 6 nm ZrO_2 particles at 500°C could be confirmed by imaging, for example with TEM observations.

The observed bonding effect was combined with the use of multiple particle fractions with different sizes to achieve densely packed structures inhibiting overall shrinkage. This approach allows the preparation of porous, well adhering ceramic coatings on rigid substrates with strength values sufficient for applications with limited requirements on the strength. It opens the way to new applications because a large variety of substrates can be equipped with such coatings via simple wet coating processes using suspensions and subsequent heating at moderate temperatures as 500°C.

For the development of new applications for those coatings it seems to be promising to apply further research effort. This will utilise the described principles for the realization of other ceramic systems. It also seems to be realistic to achieve further optimization of coating strength, density and thickness.

This work was presented at the 10th International Conference of the European Ceramic Society, June 17 - 21, 2007, Berlin and can be cited as:

J. Adam, M. Aslan, R. Drumm, M. Veith "Mechanisms of Bonding Effected by Nanoparticles in Zirconia Coatings Applied by Spraying of Suspensions" Proc. 10^{th} ECerS Conf. (2007), edited by J.G. Heinrich and C.G. Aneziris, Göller Verlag, Baden-Baden, pp. 307-311.

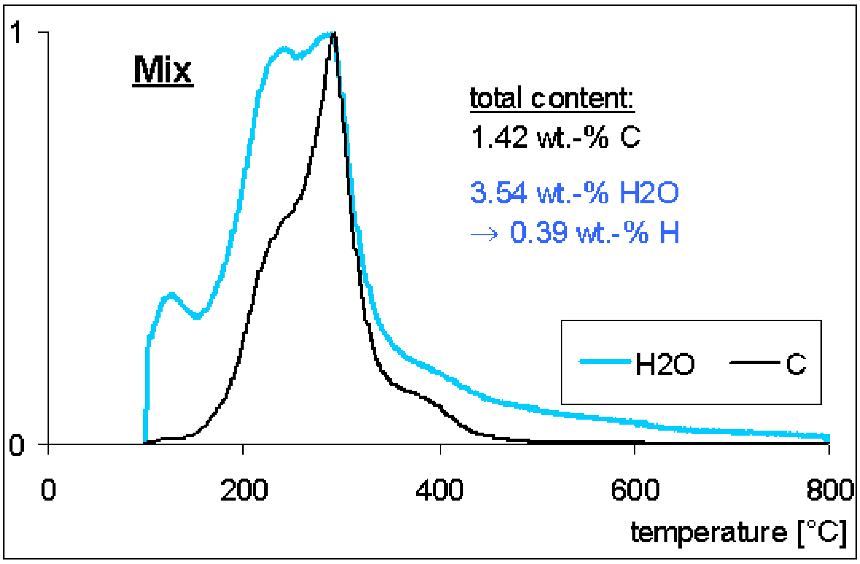

Fig. 4: Temperature dependent C and H_2O release from the mix, normalized signal (see text for specification of mix).

Preparation of Acoustic Lenses by Mechanochemical Synthesis and Electrophoretic Deposition of Lead Zirconium Titanate (PZT) Films

M. Bender, R. Drumm, J. Adam, A. Jakob*, R. Lemor*, M. Veith

References

[1] H. Salmang, H. Scholze, R. Telle (ed.): Keramik. Springer, Berlin, Heidelberg (2007)

[2] W. Lan, P. Xiao: Drying stress of yttria-stabilized-zirconia slurry on a metal substrate. J. European Ceramic Soc. 27 (2007) 3117-3125

[3] X. Wang, W.H. Lan, P. Xiao: Fabrication of yttria stabilized zirconia coatings by a novel slurry method. Thin Solid Films 494 (2006) 263-267

[4] M. Aslan, J. Adam, B. Reinhard, M. Veith: Preparation of thick zirconia coatings by spraying of colloidal suspensions. Proceedings of the 10th International Conference and Exhibition of the European Ceramic Society, 17.-21. June 2007 in Berlin

[5] M.J.M. Akash: Zr surface diffusion in tetragonal yttria stabilised zirconia. J. Materials Science 35 (2000) 437-442

[6] G. Skandan: Processing of nanostructured zirconia ceramics. NanoStructured Materials 5 (1995) 111-126

[7] W. Li, L. Gao: Compacting and sintering behaviour of nano ZrO2 powders. Scripta materialia 44 (2001) 2269-2272

[8] J. Rankin, B.W. Sheldon: In situ TEM sintering of nano-sized ZrO2 particles. Materials Science and Engineering A204 (1995) 48-53

[9] E. Mamontov: Dynamics of surface water in ZrO2 studied by quasielastic neutron scattering. J. Chemical Physics 121 (2004) 9087-9097

[10] G. Cerrato, S. Bordiga, S. Barbera, C. Morterra: Surface characterization of monoclinic ZrO2, I. Morphology, FTIR spectral features, and computer modelling. Applied Surface Science 115 (1997) 53-65

[11] H. Schmidt, K.-P. Schmitt, K. Schmitt, F. Tabellion: Method for production of nanoparticles with custom surface chemistry and corresponding colloids. Patent application WO 2006037591 A3 (priority: 2004)

Preparation of Acoustic Lenses by Mechanochemical Synthesis and Electrophoretic Deposition of Lead Zirconium Titanate (PZT) Films

(*): IBMT - Fraunhofer-Institut für Biomedizinische Technik, 66386 St. Ingbert

Abstract

PZT powder has been synthesized via reactive dry milling using $PbZrO_3$ and $PbTiO_3$ as starting materials. Stable suspensions of the PZT particles in ethanol (d_{50}(Vol) = 115 nm) were obtained by a chemomechanical disper-